receptor for clathrin AP-2: implications for membrane recycling. *Cell* **78,** 751–760 (1994).
18. Jorgensen, E. M. *et al.* Defective recycling of synaptic vesicles in synaptotagmin mutants of *Caenorhabditis elegans*. *Nature* **378,** 196–199 (1995).
19. Reist, N. E. *et al.* Morphologically docked synaptic vesicles are reduced in *synaptotagmin* mutants of *Drosophila*. *J. Neurosci.* **18,** 7662–7673 (1998).
20. Kee, Y. & Scheller, R. H. Localization of synaptotagmin-binding domains on syntaxin. *J. Neurosci.* **16,** 1975–1981 (1996).
21. Earles, C. A., Bai, J., Wang, P. & Chapman, E. R. The tandem C2 domains of synaptotagmin contain redundant Ca^{2+} binding sites that cooperate to engage t-SNAREs and trigger exocytosis. *J. Cell Biol.* **154,** 1117–1123 (2001).
22. Fernandez-Chacon, R. *et al.* Synaptotagmin I functions as a calcium regulator of release probability. *Nature* **410,** 41–49 (2001).
23. Robinson, I. M., Ranjan, R. & Schwarz, T. L. Synaptotagmins I and IV promote transmitter release independently of Ca^{2+} binding in the C_2A domain. *Nature* advance online publication, 7 July 2002 (doi:10.1038/nature00915).
24. Garcia, R. A., Forde, C. E. & Godwin, H. A. Calcium triggers an intramolecular association of the C2 domains in synaptotagmin. *Proc. Natl Acad. Sci. USA* **97,** 5883–5888 (2000).
25. DiAntonio, A., Parfitt, K. D. & Schwarz, T. L. Synaptic transmission persists in *synaptotagmin* mutants of Drosophila. *Cell* **73,** 1281–1290 (1993).
26. Del Castillo, J. & Katz, B. Quantal components of the end-plate potential. *J. Physiol.* **124,** 560–573 (1954).
27. Davletov, B. A. & Sudhof, T. C. A single C_2 domain from synaptotagmin I is sufficient for high affinity Ca^{2+}/phospholipid binding. *J. Biol. Chem.* **268,** 26386–26390 (1993).
28. Littleton, J. T., Bellen, H. J. & Perin, M. S. Expression of synaptotagmin in *Drosophila* reveals transport and localization of synaptic vesicles to the synapse. *Development* **118,** 1077–1088 (1993).

Supplementary Information accompanies the paper on *Nature*'s website (http://www.nature.com/nature).

Acknowledgements

We thank S. Royer, C. Williams and K. Mace for technical assistance, and R. Handa, K. Beam, J. Herbers, M. Tamkun and R. Aldrich for discussions about this manuscript. This work was supported by the National Science Foundation (N.E.R.), the Muscular Dystrophy Association (N.E.R.), the March of Dimes (N.E.R.) and an MRC Career Development Award (I.M.R.).

Competing interests statement

The authors declare that they have no competing financial interests.

Correspondence and requests for materials should be addressed to N.E.R. (e-mail: reist@lamar.colostate.edu).

Calorie restriction extends *Saccharomyces cerevisiae* lifespan by increasing respiration

Su-Ju Lin*, Matt Kaeberlein*†, Alex A. Andalis‡, Lori A. Sturtz§, Pierre-Antoine Defossez*†, Valeria C. Culotta§, Gerald R. Fink‡ & Leonard Guarente*

* *Department of Biology, Massachusetts Institute of Technology, Cambridge, Massachusetts 02139, USA*
‡ *Whitehead Institute for Biomedical Research, Massachusetts Institute of Technology, Cambridge, Massachusetts 02142, USA*
§ *Department of Environmental Health Sciences, Johns Hopkins University School of Public Health, Baltimore, Maryland 21205, USA*

Calorie restriction (CR) extends lifespan in a wide spectrum of organisms and is the only regimen known to lengthen the lifespan of mammals[1–4]. We established a model of CR in budding yeast *Saccharomyces cerevisiae*. In this system, lifespan can be extended by limiting glucose or by reducing the activity of the glucose-sensing cyclic-AMP-dependent kinase (PKA)[5]. Lifespan extension in a mutant with reduced PKA activity requires Sir2 and NAD (nicotinamide adenine dinucleotide)[5]. In this study we explore how CR activates Sir2 to extend lifespan. Here we show that the shunting of carbon metabolism toward the mitochondrial tricarboxylic acid cycle and the concomitant increase in respiration play a central part in this process. We discuss how this metabolic strategy may apply to CR in animals.

Ageing in yeast is regulated by *SIR2*. Deletion of *SIR2* shortens lifespan and overexpression of *SIR2* extends lifespan[6]. Sir2 exhibits an NAD-dependent histone deacetylase activity that is conserved among Sir2-family members and is required for chromatin silencing and lifespan extension[7–9]. Recent studies show that *Caenorhabditis elegans* carrying extra copies of the *SIR2* orthologue, *sir-2.1*, also exhibit a longer lifespan[10]. The unusual NAD-requirement for the Sir2 deacetylase may link metabolic rate to silencing and lifespan[11].

Calorie restriction can be modelled in yeast by reducing the glucose content of the media from 2% to 0.5% (ref. 5). We first extended our earlier findings by testing whether Sir2 is required for the extension of replicative lifespan by 0.5% glucose. As shown in Fig. 1a, growth in 0.5% glucose extended lifespan (~25% increase) relative to the normal 2% glucose, and deletion of *SIR2* prevented this extension. We also examined whether Sir2-dependent ribosomal DNA silencing is increased. As shown in Fig. 1d, cells grown on 0.5% glucose medium exhibited enhanced silencing (using a *MET15* marker integrated at the ribosomal DNA[12] as an indicator). This enhanced silencing, like the extension of lifespan on 0.5% glucose, required Sir2 function.

How does CR increase Sir2 activity and extend lifespan? As shown in Fig. 2a, glucose is metabolized to pyruvate, at which point the pathway bifurcates into respiration and fermentation[13]. Respiration oxidizes the glucose to CO_2 generating 28 ATP molecules per molecule of glucose, whereas fermentation to ethanol generates only two ATP molecules per molecule of glucose[14]. When glucose levels are high, energy is in excess and fermentation is preferred. When glucose is limiting, respiration is preferred and carbon is shunted to the mitochondrial tricarboxylic acid (TCA) cycle, thereby increasing electron transport and respiration[13].

To investigate whether this metabolic shift toward respiration occurs under our conditions of CR, we measured oxygen consumption rates of cells in 0.5% glucose. Figure 2b shows that respiration of cells grown in 0.5% glucose was significantly increased (~2-fold) compared to that of cells grown in 2% glucose. As a further test for this metabolic shift, we used a strain lacking *HXK2*, which encodes one of three hexokinases that introduce glucose into glycolysis. Deletion of *HXK2* is expected to mimic the effect of growth in low glucose and has been shown to extend lifespan[5]. Transcriptional profiling of the yeast genome indicates a highly significant overlap ($P = 3 \times 10^{-118}$) in the transcriptional changes caused by growth in 0.5% glucose and by deletion of *HXK2* (Fig. 3a). Similar to growth in 0.5% glucose, deletion of *HXK2* also increased the respiration rate significantly (~3-fold) (Fig. 2b).

Is the metabolic shift toward respiration required for CR-mediated lifespan extension? If so, elimination of electron transport ought to prevent the extension in lifespan. Thus, the gene encoding cytochrome c1, *CYT1*, was deleted, and lifespan analysis was performed (Fig. 2c). Calorie restriction failed to extend lifespan in the *cyt1Δ* mutant, suggesting that the metabolic shift toward respiration is necessary for lifespan extension mediated by CR.

We then investigated whether the metabolic shift toward respiration is sufficient for increased lifespan. Overexpression of the transcription factor Hap4 has been shown to cause a switch of metabolism from fermentation toward respiration[15]. Hap4 is expected to activate many genes involved in mitochondrial respiration[16,17]. Transcription profiling indeed showed that many of the genes that were upregulated more than 2-fold by Hap4 overexpression fell into this category (Fig. 3c; Supplementary Information Table 2). Overexpression of Hap4 significantly extended the lifespan (~35% increase) of cells grown in 2% glucose (Fig. 1b). Similar to CR, this extension required Sir2 (Fig. 1b). Hap4 overexpression also

† Present addresses: Longenity Inc., Medford, Massachusetts 02155, USA (M.K.); and CNRS UMR 5665, Ecole Normale Superieure de Lyon, France (P.-A.D.).

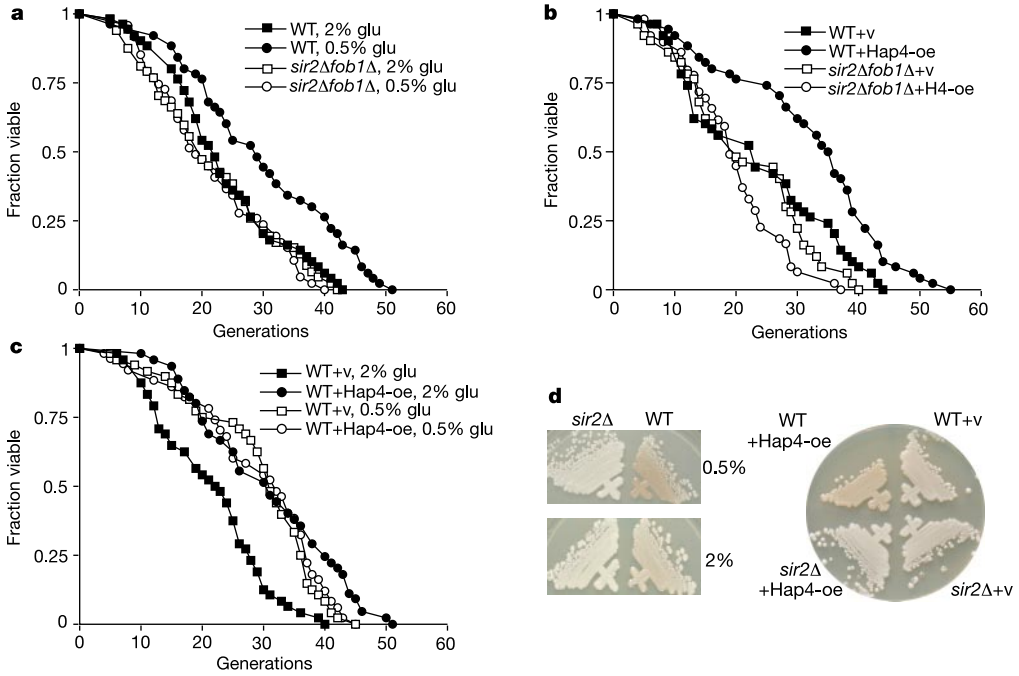

Figure 1 Calorie restriction (CR) and Hap4 overexpression extend lifespan and enhance rDNA silencing in a Sir2-dependent manner. **a**, Lifespan analysis of cells grown on media containing 0.5% and 2% glucose (glu). In 2% glucose, average lifespans in numbers of cell divisions: wild type (WT), 23.3; *sir2Δfob1Δ*, 21.5. In 0.5% glucose, average lifespans: WT, 29.4; *sir2Δfob1Δ*, 21.3. **b**, Lifespan analysis of wild-type and *sir2Δfob1Δ* mutant cells overexpressing Hap4. Average lifespans: WT + v, 23.2; WT + Hap4-oe, 31.9; *sir2Δfob1Δ* + v, 21.5; *sir2Δfob1Δ* + Hap4-oe, 19.6. The short lifespan of a *sir2ΔFOB1* strain was also unaffected by CR or by Hap4 overexpression (not shown). **c**, Lifespan analysis of cells overexpressing Hap4 on media containing 0.5% and 2% glucose. In 2% glucose, average lifespans: WT + v, 21.3; WT + Hap4-oe, 30.6. In 0.5% glucose, average lifespans: WT + v, 29.1; WT + Hap4-oe, 29. For **a**, **b** and **c**: WT indicates PSY316 wild-type cells; +v indicates cells carrying a control vector; +Hap4-oe indicates cells overexpressing Hap4; *sir2Δfob1Δ* represents an isogenic derivative of PSY316. **d**, Silencing of a *MET15* marker at the rDNA locus. Accumulation of brown pigment indicates increased silencing. Left panels, cells were streaked onto rich medium containing 0.1% $PbNO_3$ and 0.5% (top) or 2% (bottom) glucose then grown for 5 d at 30 °C. Right panel, cells were streaked onto rich medium containing 0.1% $PbNO_3$ and 2% glucose then grown for 5 d at 30 °C. WT indicates JS237 wild-type cells; +v indicates cells carrying a control vector; +Hap4-oe indicates cells overexpressing Hap4; *sir2Δ* indicates JS218, an isogenic derivative of JS237.

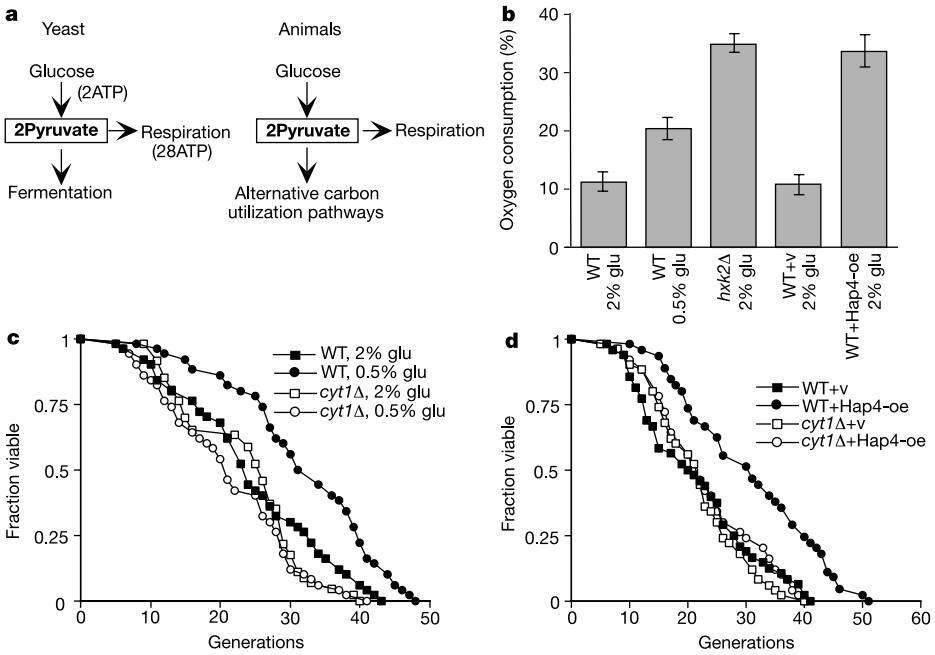

Figure 2 Respiration is required for calorie restriction (CR) and Hap4-overexpression-mediated lifespan extension. **a**, Schematic presentation of glucose utilization. During glycolysis, two molecules of pyruvate and ATP are generated per molecule of glucose, whereas respiration yields 28 ATP molecules per molecule of glucose. In mammals, pyruvate is dissimilated by respiration. In both systems, pyruvate is also used through alternative pathways such as synthesis of fatty acid and storage carbohydrates. **b**, Oxygen consumption measurement. Cells were grown in 2% or 0.5% glucose then assayed with 2% or 0.5% glucose respectively as substrates. Results shown here represent the average of 2 or 3 experimental trials, conducted in triplicate. Error bars show standard deviations. **c**, Deletion of *CYT1* prevents lifespan extension by CR. In 2% glucose, average lifespans: WT, 24.1; *cyt1Δ*, 23.3. In 0.5% glucose, average lifespans: WT, 31.9; *cyt1Δ*, 21. **d**, Deletion of *CYT1* prevents lifespan extension by Hap4 overexpression. Average lifespans: WT + v, 21; WT + Hap4-oe, 30.6; *cyt1Δ* + v, 21.5; *cyt1Δ* + Hap4-oe, 23. For **b**, **c** and **d**: WT indicates PSY316 wild-type cells; +v indicates cells carrying a control vector; +Hap4-oe indicates cells overexpressing Hap4; *cyt1Δ* and *hxk2Δ* represent isogenic derivatives of PSY316.

increased Sir2-dependent rDNA silencing (Fig. 1d). Thus, shifting metabolism toward respiration in cells grown in 2% glucose is sufficient to trigger the same effects on lifespan and silencing as does CR.

Three further findings reinforce the conclusion that the shift toward respiration induced by CR and by Hap4 overexpression is what extends lifespan. First, Hap4 overexpression did not synergize with growth on 0.5% glucose for the extension of lifespan (Fig. 1c). Second, Hap4 overexpression failed to extend lifespan in a respiration-deficient *cyt1Δ* mutant (Fig. 2d). Third, Hap4 overexpression resulted in a substantial increase in the respiration rate (~3-fold), similar to the increase observed for the *hxk2Δ* mutant (Fig. 2b).

We also compared the transcriptional effects of Hap4 overexpression to CR (the 124 genes co-regulated by 0.5% glucose and *hxk2* mutant; Supplementary Information Table 1). As shown in Fig. 3b, of the 255 genes upregulated more than 2-fold by Hap4 overexpression (Supplementary Information Table 2), 55 genes were similarly regulated by CR (Supplementary Information Table 3). This overlap is statistically significant ($P = 1.5 \times 10^{-33}$). However, many of the transcriptional changes observed by overexpressing Hap4 were not observed during CR, and in fact, *HAP4* gene expression is not induced by CR. These observations suggest that transcriptional mechanisms unrelated to Hap4 or post-transcriptional mechanisms may also contribute to the activation of respiration by CR.

Other studies have suggested that CR functions to extend lifespan by increasing resistance to reactive oxygen species (ROS) and/or by reducing the production of ROS[3]. It thus seemed possible that the shift toward respiration under CR could extend lifespan by inducing resistance to ROS. However, expression of most antioxidant genes was not increased by Hap4 overexpression or by CR (Fig. 4a; Supplementary Information Table 4). Because a few genes, such as *SOD2* (mitochondrial superoxide dismutase), were slightly upregulated by Hap4 overexpression, we directly investigated whether CR or Hap4 overexpression increases resistance to oxidative stress. As shown in Fig. 4b, both CR and Hap4 overexpression, if anything, resulted in a slight decrease in resistance to paraquat. Further, while deletion of *SOD2* conferred a high degree of sensitivity to paraquat, deletion of *SIR2* had no effect. Also shown in Fig. 4c, CR and Hap4 overexpression slightly decreased resistance to hydrogen peroxide. As a control, deletion of *YAP1* gave rise to hypersensitivity to hydrogen peroxide, but, as for paraquat, deletion of *SIR2* did not. These findings all suggest that the Sir2-mediated extension of lifespan during CR is not due to an increase in resistance to oxidative stress.

How does this metabolic shift toward respiration during CR activate Sir2? First, the higher yield of ATP per input carbon allows a slower rate of glycolysis. Second, the increase in respiration yields a higher rate of electron transport, thereby increasing the re-oxidation of NADH to NAD in the mitochondria. This may increase the NAD/NADH ratio in the mitochondria, a change that can be transmitted to the cytosol by a shuttle that moves redox equivalents across the mitochondrial membrane[18]. It seems that the generation of NAD in the mitochondria is important, because disruption of the electron transport chain prevents the extension in lifespan by CR. Thus, we infer that the slowing of carbon flow through glycolysis, an increase in the NAD/NADH ratio, or both, contribute to the activation of Sir2 and the extension of lifespan.

Because CR in yeast does not increase resistance to oxidative stress, ROS are not limiting for the replicative lifespan of mother cells and are not central to the extension of lifespan by CR. ROS do, however, limit the long-term survival of stationary phase yeast cells[19,20], and may also play a role in the ageing of post-mitotic cells in *Drosophila melanogaster* and *C. elegans*[21–23]. It is therefore intriguing that the replicative ageing of yeast mother cells and the post-mitotic aging in *C. elegans* are both regulated by the levels of Sir2 proteins[6,10].

Our results are in contrast to the frequent suggestion that CR functions by slowing metabolism and thereby slowing the generation of ROS; in fact, data addressing whether CR actually changes the rate of respiration in animals is conflicting. In animals, respiration is essential for viability and mutations that reduce electron transport slow glycolysis and development and also lengthen lifespan[24]. This is consistent with one of our proposed mechanisms for CR in yeast, that shifting metabolism toward respiration extends the lifespan by slowing glycolysis. In mammals, major pathways of carbon utilization, other than the TCA cycle, include the synthesis of fatty acids and storage carbohydrates[13] (Fig. 2a). These alternative pathways (perhaps analogous to fermentation) are likely to be lowered to a greater degree during CR than the energy-producing TCA cycle.

We note that expression profiling of mouse skeletal muscle suggests that CR induces gluconeogenesis[25]. This change is diagnostic of cells in a state of ATP excess, consistent with the hypothesis that CR diverts a higher fraction of the carbon into the TCA cycle. Finally, the increase in anti-oxidant enzymes that is reported to occur during CR in animals may be a result of an increase in respiration rather than a cause of the observed longevity. These considerations suggest that the essence of our models for CR in yeast could apply to animals. □

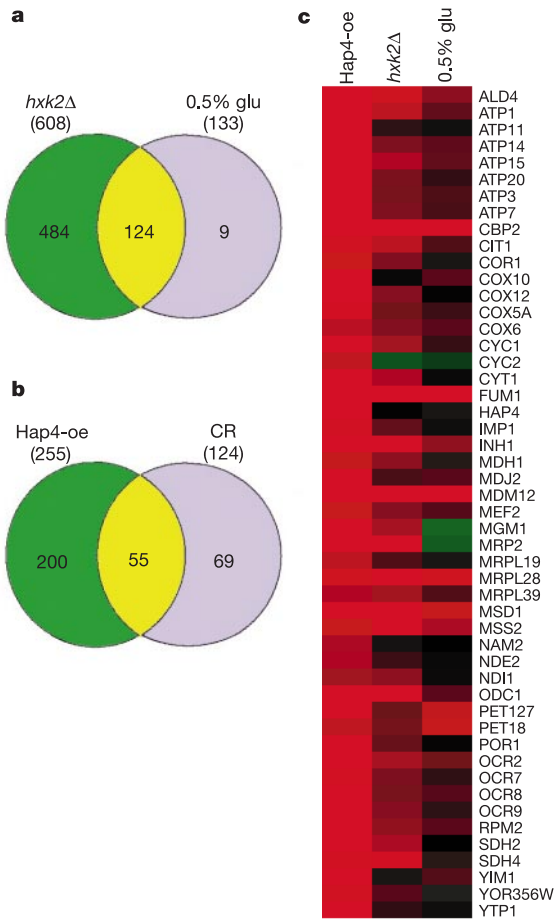

Figure 3 Gene expression profile analysis of cells under calorie restriction (CR) and overexpressing Hap4. **a**, Venn diagram of genes regulated by deletion of *HXK2* and growth in 0.5% glucose. Of the 133 genes differentially regulated by 0.5% glucose, 124 are similarly regulated by deletion of *HXK2*. **b**, Venn diagram of genes regulated by CR (0.5% glucose and *hxk2Δ*) and Hap4 overexpression (Hap4-oe). Of the 124 genes differentially regulated by CR, 55 genes are similarly regulated by overexpressing Hap4. **c**, Cluster analysis of genes regulated by CR (0.5% glucose and *hxk2Δ*) and Hap4 overexpression (Hap4-oe). Red represents genes that are upregulated and green represents genes that are downregulated.

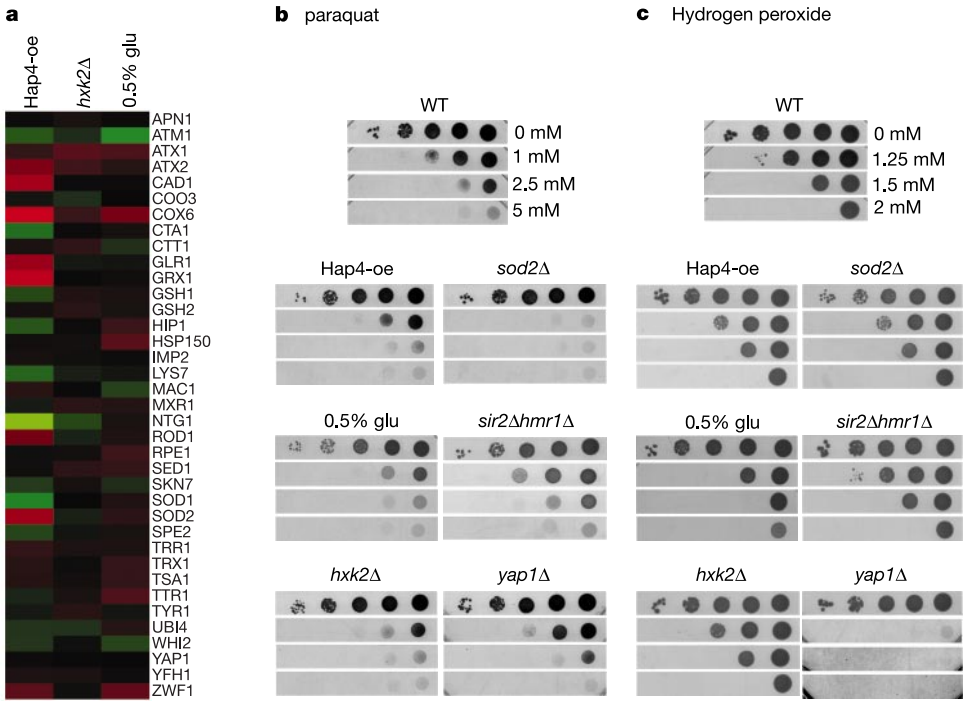

Figure 4 Calorie restriction (CR) and Hap4 overexpression do not increase the oxidative stress response. **a**, Cluster analysis of expression profile of genes involved in oxidative stress response in calorie-restricted (0.5% glucose and *hxk2Δ*) and Hap4-overexpressing (Hap4-oe) cells. Red represents genes that are upregulated and green represents genes that are downregulated. **b**, Paraquat sensitivity tests. **c**, Hydrogen peroxide sensitivity tests. For **b** and **c**, serial 10-fold dilutions of cells were spotted onto synthetic complete media containing different concentrations of paraquat or hydrogen peroxide then grown at 30 °C for 2 d. The *HMR1* gene was deleted in the *sir2Δ* mutant to eliminate mating type effects. WT indicates PSY316 wild type; Hap4-oe indicates WT cells overexpressing Hap4; *hxk2Δ*, *sod2Δ*, *sir2Δhmr1Δ* and *yap1Δ* represent isogenic derivatives of PSY316.

Methods

Strains and plasmids

Strains PSY316 (*MAT*α, *ura3-52*, *leu2-3, 112*, *his3-Δ200*, *ade2-101*, *lys2-801*, *RDN1::ADE2*), JS237 (*MAT*α, *his3Δ200*, *met15Δ1*, *ura3-167*, *leu2Δ1*, *RDN1::Ty1-met15*) and JS218 (*MAT*α, *his3Δ200*, *met15Δ1*, *ura3-167*, *leu2Δ1*, *RDN1::Ty1-met15*, *sir2Δ::HIS3*) have been previously described[5,12].

The integrating ppp81 (*LEU2*) vector, which allows gene overexpression under an *ADH1* promoter, was provided by P. Park. The Hap4 overexpression construct p*ADH1-HAP4* was made as follows: a pair of oligo-nucleotides were designed to amplify the *HAP4* coding region (from start codon to stop codon) by polymerase chain reaction (PCR) using Pfu DNA polymerase. This pair of oligo-nucleotides also added a *Not*1 site to the 5′ end and a *Nhe*1 site to the 3′ end of the *HAP4* gene. After PCR amplification, DNA was digested with *Not*1 and *Nhe*1, then ligated to ppp81 digested with the same enzymes resulting in p*ADH1-HAP4*. DNA sequencing analysis of p*ADH1-HAP4* showed that no mutation was introduced into the *HAP4* gene during PCR amplification. This construct was further verified by its ability to suppress the growth defects of a *hap4Δ* mutant on non-fermentable carbon.

WT + Hap4-oe strains were made by integrating *Xcm*1 linearized p*ADH1-HAP4* into the *LEU2* locus. WT + v strains were made by integrating *Xcm*1 linearized ppp81 into the *LEU2* locus. All gene deletions in this study were constructed by replacing the wild-type genes with the *Kan*^{r} marker as described[26], and verified by PCR using oligo-nucleotides flanking the genes of interest.

Lifespan, silencing and paraquat sensitivity assays

Lifespan analyses were carried out as previously described[5]. All lifespan analyses in this study were carried out on YPD plates at least twice independently with more than 45 cells per strain per experiment. Results from a single experiment are shown.

Silencing assays were carried out by streaking cells onto YPD media containing 0.1% $PbNO_3$ and 2% or 0.5% glucose, then grown for 5 d at 30 °C. Serial dilution assays were performed by growing cells overnight in YPD at 30 °C. Cells were then diluted 50-fold in fresh YPD and cultured for 4–5 h. For each strain, a series of 10-fold dilutions were prepared in fresh synthetic media over a range of concentrations from 10^{-1} to 10^{-5}, relative to the initial culture. 5 μl of the original culture and each dilution were spotted sequentially onto the appropriate media. The cells were then grown at 30 °C for 2 d before visualization. Paraquat media were prepared by supplementing synthetic complete media with 0, 1, 2.5, or 5 mM paraquat (Methyl Viologen, Sigma). Hydrogen peroxide media were prepared by supplementing synthetic complete media with 0, 1.25, 1.5, 2 mM hydrogen peroxide (H_2O_2, Sigma).

Oxygen consumption assay

For oxygen consumption experiments, cells were first grown overnight in YPD media containing either 2% or 0.5% glucose, then diluted into fresh media the next day. For cells grown in 2% glucose, cultures were diluted to an optical density at 600 nm (OD_{600}) of 0.2. Cells grown in 0.5% glucose were diluted to $OD_{600} = 0.05$. Growth of cultures was continued at 30 °C with shaking for approximately 6–8 h until the final OD_{600} of cultures grown in 2% glucose was 0.8 and that of cultures grown in 0.5% glucose was 0.2. Cells were then harvested, washed and resuspended in 500 μl of fresh YPD media containing either 2% or 0.5% glucose. Oxygen consumption was measured using a YSI Model 5300 Biological Oxygen Monitor equipped with a Clark-type oxygen electrode (Yellow Springs Instrument) and readings were recorded every 15 s. For WT + v and WT + Hap4-oe strains, 2.5×10^8 cells were assayed. For WT cells grown in 2% and 0.5% glucose and the *hxk2Δ* strain, 1.0×10^8 cells were used. Results are reported as per cent O_2 consumed per minute per 1×10^9 cells.

Microarray analysis

Slides for microarray analysis were prepared by PCR amplification of yeast open reading frames (ORFs) using the Research Genetics Yeast Gene Pairs primer set. All ORFs were spotted onto glass slides coated with poly-L-lysine using a Genemachines Omnigrid Microarrayer and post-processed[27].

To obtain messenger RNA for microarray analysis, cells were grown in YPD overnight and diluted 100-fold into fresh YPD and incubated at 30 °C to an OD_{600} between 0.6 and 0.8. For cells grown in low glucose, cultures were incubated overnight in YPD containing 0.5% glucose then diluted 250-fold and grown to $OD_{600} = 0.2$. Cells were then washed in water and frozen in dry ice/ethanol before storage at −80 °C.

Total RNA was obtained by the acid-phenol method. mRNA was purified from total RNA using the PolyATtract mRNA isolation system (Promega). 2 μg of mRNA was labelled for each sample using the reverse transcription and amino-allyl coupling method described at http://www.microarrays.org. Reference samples of wild-type PSY316 mRNA harvested from cells grown in YPD at 30 °C were labelled with Cy3 and experimental samples were labelled with Cy5. Labelled samples were combined and hybridized overnight at 42 °C. After hybridization, slides were washed[27] and scanned using a Packard BioScience 3000 scanner. Images were processed using the MolecularWare DigitalGENOME (Cambridge, MA) software package. All microarray data sets are available as Microsoft Excel files at http://web.mit.edu/biology/guarente/arrays/kaeberlein.

A scaling factor was calculated and applied in each microarray experiment so that the median ratio value of all experiments was equal to 1. Genes were defined as differentially regulated if the Cy5/Cy3 ratio was greater than 1.5 or less than 0.667 (−1.5-fold) in both of two independent experiments. Reported values are the mean values of duplicate experiments. For the *HXK2* deletion, a single microarray experiment was performed. Cluster analysis was performed using Cluster and visualized with TreeView[28]. Red represents genes that are upregulated and green represents genes that are downregulated. Statistical significance of the overlap between regulated genes in different experiments

shown in Fig. 3 was calculated using a hypergeometric distribution. *P*-values were obtained from the online hypergeometric distribution calculator at http://www.alewand.de/stattab/tabdiske.htm.

Received 8 March; accepted 12 April 2002; doi:10.1038/nature00829.

1. Weindruch, W. & Walford, R. L. *The Retardation Of Aging And Diseases By Dietary Restriction* (Thomas, Springfield, Illinois, 1998).
2. Roth, G. S., Ingram, D. K. & Lane, M. A. Calorie restriction in primates: will it work and how will we know? *J. Am. Geriatr. Soc.* **47,** 896–903 (1999).
3. Sohal, R. S. & Weindruch, R. Oxidative stress, caloric restriction, and aging. *Science* **273,** 59–63 (1996).
4. Yu, B. P. *Modulation of Aging Processes by Dietary Restriction* (CRC Press, Boca Raton, Florida, 1994).
5. Lin, S. J., Defossez, P. A. & Guarente, L. Requirement of NAD and *SIR2* for life-span extension by calorie restriction in *Saccharomyces cerevisiae*. *Science* **289,** 2126–2128 (2000).
6. Kaeberlein, M., McVey, M. & Guarente, L. The *SIR2/3/4* complex and *SIR2* alone promote longevity in *Saccharomyces cerevisiae* by two different mechanisms. *Genes Dev.* **13,** 2570–2580 (1999).
7. Smith, J. S. *et al.* A phylogenetically conserved NAD^+-dependent protein deacetylase activity in the Sir2 protein family. *Proc. Natl Acad. Sci. USA* **97,** 6658–6663 (2000).
8. Landry, J. *et al.* The silencing protein *SIR2* and its homologs are NAD-dependent protein deacetylases. *Proc. Natl Acad. Sci. USA* **97,** 5807–5811 (2000).
9. Imai, S., Armstrong, C. M., Kaeberlein, M. & Guarente, L. Transcriptional silencing and longevity protein Sir2 is an NAD-dependent histone deacetylase. *Nature* **403,** 795–800 (2000).
10. Tissenbaum, H. A. & Guarente, L. Increased dosage of a *sir-2* gene extends lifespan in *Caenorhabditis elegans*. *Nature* **410,** 227–230 (2001).
11. Guarente, L. Sir2 links chromatin silencing, metabolism, and aging. *Genes Dev.* **14,** 1021–1026 (2000).
12. Smith, J. S. & Boeke, J. D. An unusual form of transcriptional silencing in yeast ribosomal DNA. *Genes Dev.* **11,** 241–254 (1997).
13. Pronk, J. T., Yde Steensma, H. & Van Dijken, J. P. Pyruvate metabolism in *Saccharomyces cerevisiae*. *Yeast* **12,** 1607–1633 (1996).
14. Stryer, L. *Biochemistry* (Freeman, New York, 1995).
15. Blom, J., De Mattos, M. J. & Grivell, L. A. Redirection of the respiro-fermentative flux distribution in *Saccharomyces cerevisiae* by overexpression of the transcription factor Hap4. *Appl. Environ. Microbiol.* **66,** 1970–1973 (2000).
16. de Winde, J. H. & Grivell, L. A. Global regulation of mitochondrial biogenesis in *Saccharomyces cerevisiae*. *Prog. Nucleic Acid Res. Mol. Biol.* **46,** 51–91 (1993).
17. Forsburg, S. L. & Guarente, L. Identification and characterization of *HAP4*: a third component of the CCAAT-bound *HAP2/HAP3* heteromer. *Genes Dev.* **3,** 1166–1178 (1989).
18. Bakker, B. M. *et al.* Stoichiometry and compartmentation of NADH metabolism in *Saccharomyces cerevisiae*. *FEMS Microbiol Rev.* **25,** 15–37 (2001).
19. Longo, V. D., Gralla, E. B. & Valentine, J. S. Superoxide dismutase activity is essential for stationary phase survival in *Saccharomyces cerevisiae*. Mitochondrial production of toxic oxygen species *in vivo*. *J. Biol. Chem.* **271,** 12275–12280 (1996).
20. Fabrizio, P., Pozza, F., Pletcher, S. D., Gendron, C. M. & Longo, V. D. Regulation of longevity and stress resistance by Sch9 in yeast. *Science* **292,** 288–290 (2001).
21. Melov, S. *et al.* Extension of life-span with superoxide dismutase/catalase mimetics. *Science* **289,** 1567–1569 (2000).
22. Orr, W. C. *et al.* Extension of life-span by overexpression of superoxide dismutase and catalase in *Drosophila melanogaster*. *Science* **263,** 1128–1130 (1994).
23. Taub, J. *et al.* A cytosolic catalase is needed to extend adult lifespan in *C. elegans daf-C* and *clk-1* mutants. *Nature* **399,** 162–166 (1999).
24. Feng, J., Bussiere, F. & Hekimi, S. Mitochondrial electron transport is a key determinant of lifespan in *Caenorhabditis elegans*. *Dev. Cell* **1,** 633–644 (2001).
25. Lee, C. K., Klopp, R. G., Weindruch, R. & Prolla, T. A. Gene expression profile of aging and its retardation by caloric restriction. *Science* **285,** 1390–1393 (1999).
26. Guldener, U., Heck, S., Fielder, T., Beinhauer, J. & Hegemann, J. H. A new efficient gene disruption cassette for repeated use in budding yeast. *Nucleic Acids Res.* **24,** 2519–2524 (1996).
27. Hegde, P. *et al.* A concise guide to cDNA microarray analysis. *Biotechniques* **29**, 548–550, 552–554, 556 (2000).
28. Eisen, M. B., Spellman, P. T., Brown, P. O. & Botstein, D. Cluster analysis and display of genome-wide expression patterns. *Proc. Natl Acad. Sci. USA* **95,** 14863–14868 (1998).

Supplementary Information accompanies the paper on *Nature*'s website (http://www.nature.com/nature).

Acknowledgements

We thank D. McNabb and members of the Guarente laboratory for suggestions; J. Smith for providing strains; T. Galitski for his contributions in the development of microarrays and analytical software tools; and T. Ideker for suggestions with microarray analysis. This work was supported by grants to L.G. from the National Institute of Health (NIH), The Ellison Medical Foundation, The Seaver Institute, and the Howard and Linda Stern Fund. S.-J.L. is supported by a NRSA individual award. G.R.F. is supported by the NIH and is an American Cancer Society Professor of Genetics. A.A.A. is supported by the NIH Training Grant in Genomic Sciences, sponsored by the Biotechnology Process Engineering Center. V.C.C. and L.A.S. are supported by grants from the NIH.

Competing interests statement

The authors declare competing financial interests: details accompany the paper on *Nature*'s website (http://www.nature.com/nature).

Correspondence and requests for materials should be addressed to L.G. (e-mail: leng@mit.edu).

Adenovirus oncoproteins inactivate the Mre11–Rad50–NBS1 DNA repair complex

Travis H. Stracker*†, Christian T. Carson*† & Matthew D. Weitzman*

* *Laboratory of Genetics, The Salk Institute for Biological Studies, La Jolla, California 92037, USA*
† *Graduate Program, Department of Biology, University of California, San Diego, California 92093, USA*

In mammalian cells, a conserved multiprotein complex of Mre11, Rad50 and NBS1 (also known as nibrin and p95) is important for double-strand break repair, meiotic recombination and telomere maintenance[1–4]. This complex forms nuclear foci and may be a sensor of double-strand breaks. In the absence of the early region E4, the double-stranded DNA genome of adenovirus is joined into concatemers too large to be packaged[5,6]. We have investigated the cellular proteins involved in this concatemer formation

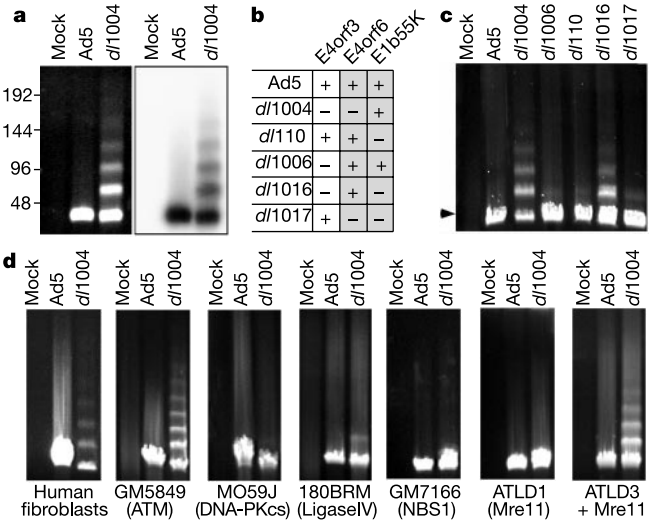

e

Cell line	Mutant	CF
HeLa	–	+
A549	–	+
MO59K	–	+
MCF7	–	+
HCC1937	BRCA1	+
GM5849	ATM	+
GM1740	ATM	+
Saos2	p53	+
GM1492G	BLM	+
AG780H	WRN	+

Cell line	Mutant	CF
MO59J	DNA-PKcs	–
180BRM	LigaseIV	–
ATLD1	Mre11	–
ATLD3	Mre11	–
GM7166	NBS1	–
GM7166A	NBS1	–
ATLD3/M	+Mre11	+
GM7166/N	+NBS1	+

Figure 1 Adenovirus genome concatemer formation with wild-type (Ad5) and mutant viruses in human cell lines. **a**, Concatemers of Ad genomes. HeLa cells were either uninfected (mock) or infected with wild-type Ad5 or an E4-deleted virus (*dl*1004) at an MOI of 25 p.f.u. per cell. DNA was prepared at 30 h.p.i. and analysed by PFGE. Left, gel stained with ethidium bromide with the positions of size markers indicated in kilobases. Right, Southern blot hybridization with an Ad probe. **b**, Genotype of mutant adenoviruses used for infections. Shading indicates that the E4orf6 and E1b55K proteins function as a complex. **c** Concatemer formation is observed when both E4orf3 and the E4orf6–E1b55K complex are inactivated. HeLa cells were infected with mutant viruses and analysed by PFGE. The position of the single linear viral genome is indicated. **d**, Cellular requirements for concatemer formation. Wild-type and mutant cell lines were infected with viruses and DNA was analysed by PFGE. Mutated genes are indicated in parentheses. **e**, Summary of concatemer formation (CF) in mutant cell lines. Reconstituted cell lines are shown at the bottom.